

Post-Stack Reflectivity Inversion for Hydrocarbon Prospectivity in the Niger Delta Field

Ekone, N.O¹; Ehirim, C. N.²; Nwosu, J.I.³ and Dagogo, T.².

¹World Bank Africa Centre of Excellence (Centre For Oilfield Chemical Research), University Of Port Harcourt.

²Department of Physics, University of Port Harcourt, Nigeria.

³Department of Geology, University of Port Harcourt

Abstract: The present study describes the use of seismic inversion process to optimize the reservoir characterization of a field in the Niger Delta basin of Nigeria. The purpose of the study was to use post-stack reflectivity inversion to predict the lithology, porosity and presence hydrocarbon within the field away from well control. The reservoir interval were discriminated and evaluated to show characterize lithology and identified fluid. The estimated average porosity in B20 reservoir varies from 28% to 31% while the volume of shale and water saturation ranges from 6% to 8% and 19% to 27% in Niger Delta reservoir respectively. The inversion result and the RMS attribute was used to predict lithology variation in the field. The sand facies indicate high RMS amplitude corresponding to low acoustic impedance at the top of the reservoir. Higher-quality areas of Niger Delta reservoir were spotted and specific consideration were dedicated to some deep geological structures that have favored hydrocarbon accumulation.

Keywords: Well log analysis, Structural interpretation, Acoustic impedance, Seismic inversion

Date of Submission: 08-01-2020

Date of acceptance: 23-01-2020

I. Introduction

The reflection of seismic waves from subsurface layers reveal potential hydrocarbon accumulations. As waves reflect, their amplitude change to uncover significant information about the subsurface. Petroleum geoscientists use amplitudes to foresee variation in lithology and presence of fluids (Hampson *et al.* 2001). However, extracting reservoir information poses great difficulty for seismic interpreter. Seismic inversion serves as one of the powerful tools for estimating detailed characteristics of the reservoir (Krebs *et al.*, 2009). Seismic inversion method converts the seismic reflection amplitude (reflectivity) into impedance values which is a characteristics of the geologic layer.

Inversion could be pre- or post-stack where acoustic and shear impedances and acoustic impedance are estimated, respectively. Inversion results demonstrate high resolution and diminishes the risk involve in drilling (Pendrel, 2006).

Post-stack inversion is the most used inversion method because it is fast, reliable and yields acoustic impedance property from the reflection amplitudes. Acoustic impedance is a quantitative seismic attribute used for reservoir characterization. It is closely related to lithology, porosity, pore fill and pressure. The significance of this property is that it contains greater subsurface information than seismic data (Latimare *et al.* 2000). Post stack inversion has been adopted by several authors (Ebeniro *et al.*, 2003; Adekanle and Enikanselu, 2013; Rahim *et al.*, 2014; Sinha and Mohanty 2015; Kumar *et al.*, 2016; Dagogo *et al.*, 2016; Aamire *et al.*, 2018) in reservoir characterization. Their study reveals acoustic impedance in combination with other pertinent seismic attributes are used for prediction of reservoir lithology, hydrocarbon potential prediction, as well as reservoir property estimation.

The study area is located in the eastern Niger delta, Nigeria (Figure 1). Niger delta is a basin of 12km sedimentary thickness developed by rift faulting during the Precambrian (Weber, 1971), rich in hydrocarbons. Physiographically, the region is characterized by low-lying, flat geomorphic units with dense network of meandering rivers and creeks with abundant rainfall. The vegetation is dominantly mangrove typical of the zone.

The study is aimed at integrating 3-D seismic and well data for post- stack reflectivity inversion in order to analyze reflection characteristics that are favourable to probable hydrocarbon accumulations in the field.

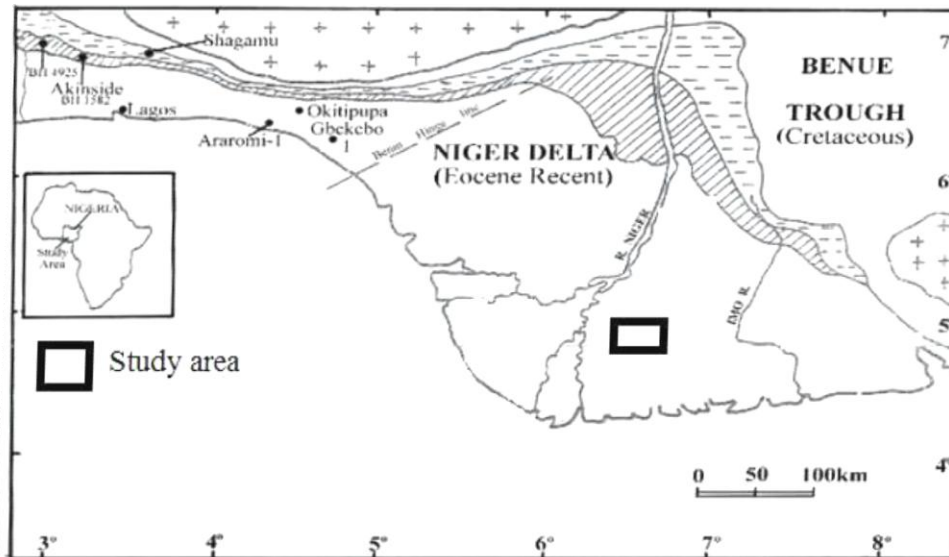


Figure 1. Location map of the study area (modifications after Petters and Olsson, 1979).

GEOLOGY OF THE STUDY AREA

The general geology knowledge of the Niger Delta have been outlined by the works of (Short and Stauble, 1967; Murat, 1970; Meki, 1970; Weber, 1971; Weber and Daukoru, 1975; Evamy *et al.*, 1978; Rider, 1996; Selley, 1997). The author view portrayed how differential stacking of under compacted shale at the base of the Tertiary delta by the moderately substantial sandy deposits resulted to the development of syndimentary fault (growth faults) and associated structural features such roll over anticlines. It is believed that the modern delta might have evolved during the Eocene era. The Niger Delta displays basin characteristics of deltaic environment encompassing marine, mixed and continental sedimentations which are represented by the Benin, Agbada and Akata Formations. An averaged segment of the Niger Delta outlining the diapiric structures on the continental slope as well as the faulting of the Oligocene and younger formations drawn by Thomas, 1999 is shown in (Figure 2),

The Benin Formation is the youngest lithostratigraphic unit in the Niger Delta. The Benin Formation overlies the Agbada Formation and is made up of high sand percentage (70–100%)

of massive continental sands. The Agbada Formation is the real oil bearing unit in the Niger Delta. It overlies the Akata Formation and consists of alternations of sand and shale layers (Pochat *et al.*, 2004). The paralic sequence aged Eocene to Pleistocene is present in all depobelts as with the marine shales. The Agbada Formation forms the hydrocarbon reservoir sequence in the Niger Delta as it contains most exploration wells.

The Akata Formation is the basal sedimentary unit of the delta. It comprises of uniform prodeltaic dark grey over-pressured marine shales with sandy turbidites and channel fills (Stacher, 1995; Doust and Omatsola, 1989). It is believed to be the main source rock of the Niger delta basin.

At the point when the throw of the fault exceeds the sand thickness, the fault zone serves as a seal however this relies upon the measure of shale spread into the fault plane. Rollover anticlines consistently happen in relationship with the growth faults and it is in these structures that oil and gas in the Agbada reservoir sands have been known (Evamy *et al.*, 1978)

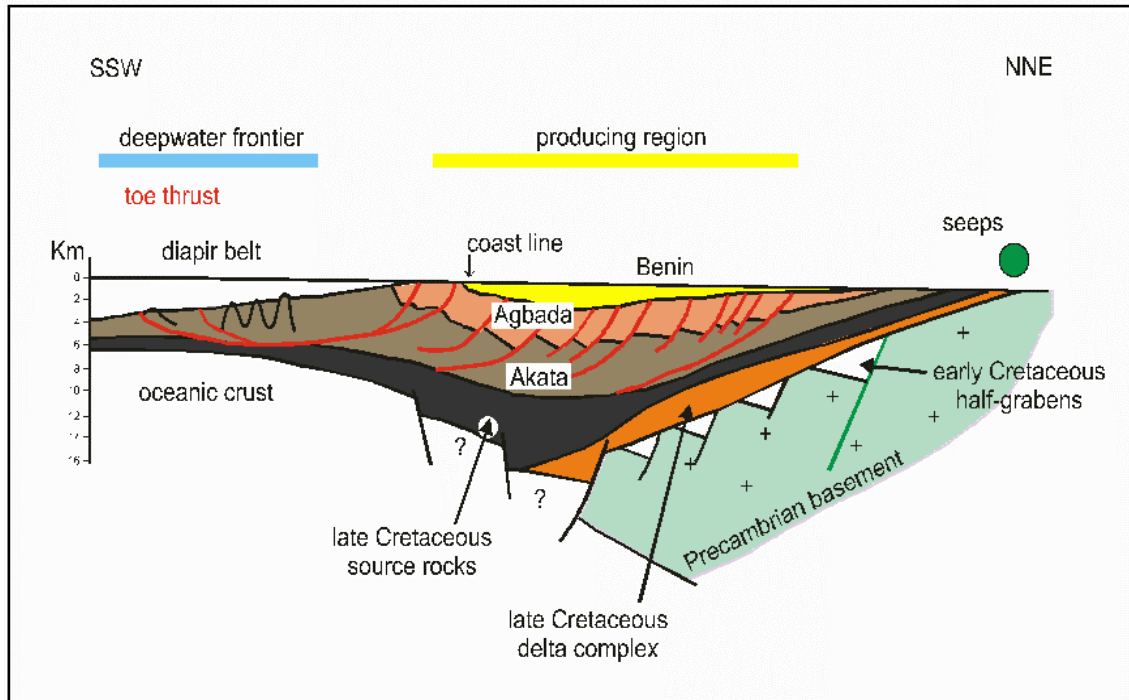


Figure 2; Geologic segment of the Niger Delta (After Thomas, 1995)

II. Material And Methodology

This study make used of a base map (Figure 3), 3D Post Stack Time Migrated (PSTM) Seismic volume and well log data to determine the prospectivity of the Niger Delta field. Three wells were considered for this study whose logs incorporate Gamma ray (GR), resistivity (LLD) and density (RHOB), sonic log and check shot data. However, only two wells EK1 and EK2 were chosen for reviewed for curve availability, editing and detailed analysis because of data quality issues. All the data files are in standard digital format and Petrel (A Schlumberger software) was used for the Interpretation. Data were extensively visualized in deciding the lithology, the shale and clean sand base lines were established from the gamma ray log. The top and base of the reservoirs (sandstone) are picked based on gamma ray value below a threshold of 100 API. The depth interval of the reservoir of interest (B20) ranges from 5800ftss and 5910ftss for the well. A combined gamma ray log and resistivity log was used for lithostratigraphic unit correlation of sand B10 to B20 based on low gamma ray counts and high electrical resistivity values (Figure 4). Petrophysical analysis was done using the following petrophysical model equations

- Gamma ray index was estimated using the $IGR = (GR_{log} - GR_{min}) / (GR_{max} - GR_{min})$

Where:

IGR is the gamma ray index

GR_{log} is the Gamma Ray Log reading of the formation

GR_{min} is the Gamma Ray for a complete sand (100% clean sand) matrix zone

GR_{max} is the Gamma Ray for a complete shale zone (100% shale)

- Volume of Shale was estimated using $V_{sh} = 0.083 * [2^{(3.7 * IGR)} - 1]$ Larionov tertiary (1969).

- The density log was used for the estimation of the total porosity by using

$PoroT = (\rho_{mat} - \rho_{bulk}) / (\rho_{mat} - \rho_{fluid})$. (Schlumberger, 1989).

Where $PoroT$ is the total porosity derived from density log, ρ_{mat} is matrix density (2.65 g/cm^3), ρ_{bulk} is bulk density and ρ_{fluid} is fluid density (1 g/cm).

- Effective porosity was estimated using $PoroE = (1 - V_{sh}) * PoroT$

- Water Saturation was estimated using the Archie Equation $S_w = [R_w * a / (R_t * PoroT^m)]^{1/n}$

Where,

R_t = true formation resistivity (Deep Resistivity)

R_w = formation water resistivity at formation temperature

a = Archie's exponent or tortuosity factor

n = Saturation exponent

F = formation factor

m = cementation exponent factor = 2

- Permeability was estimated using $K = [250 * (\text{Porosity})^3 / \text{Swirr}]^2$ (Tixier, 1949)

The 3D PSTM reflection data was analyzed for fault interpretation, horizon mapping, RMS attribute characterization and modern based inversion. The identification of faults based on mapping the seismic section for reflection discontinuities, vertical displacement of reflection events and abrupt termination of events. The synthetic seismogram was then generated from the well that has checkshot data and this was utilized to tie seismic to well data (figure 5). This tie increased the confidence in the events to be picked for horizon mapping. The exact horizons for the top of the reservoirs were picked and this ensures that the interpretation process is consistent for reflection characteristics of their terms of reflection strength, amplitude of the seismic sections. Based on the acoustic impedance inversion results, the seismic porosity transform was carried out using collocated cokriging to reveal the reservoir heterogeneity and lithology discrimination. As a final step, we compared the time and depth structural map of the horizon generated, attribute based prediction and the inversion results for identifying lithological features and hydrocarbon prospect in the study area.

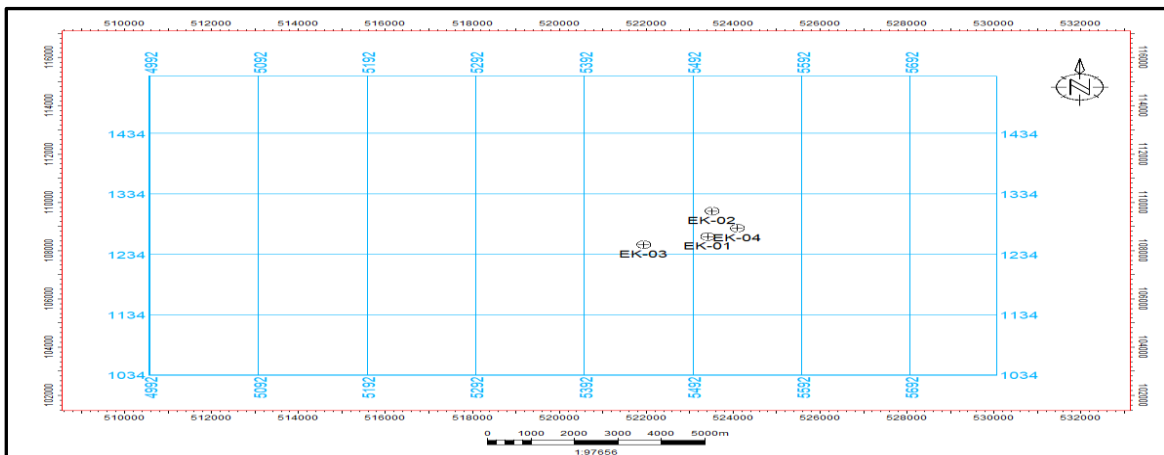


Figure 3: Seismic survey base map of the study area showing location of four wells

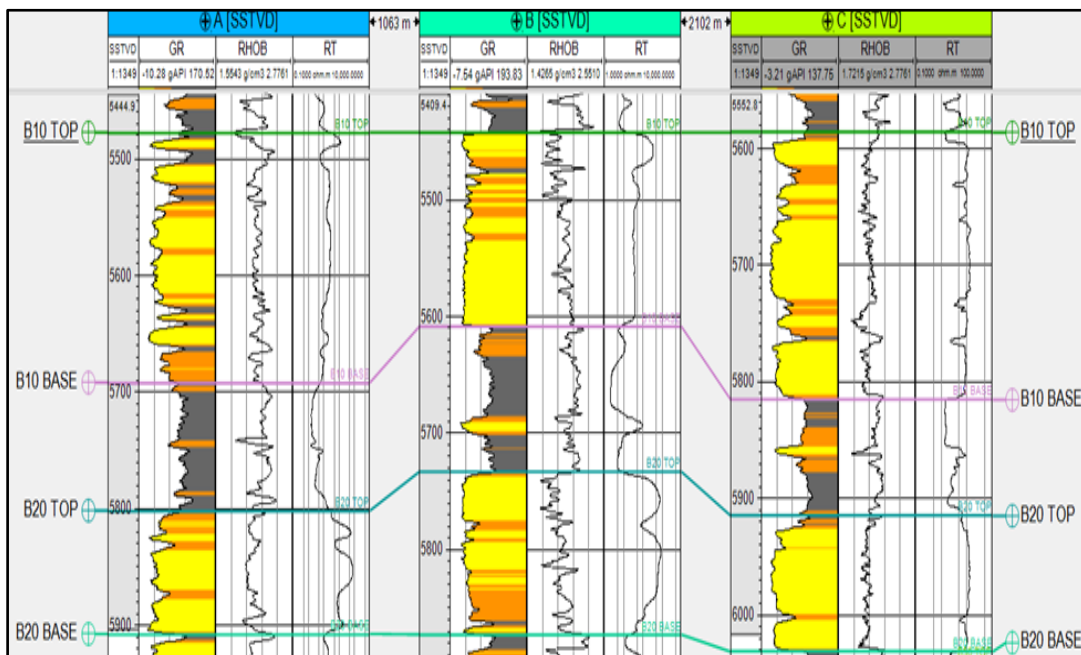


Figure 4. Showing Well Correlation panel of the study area (Sand B10 to B20)

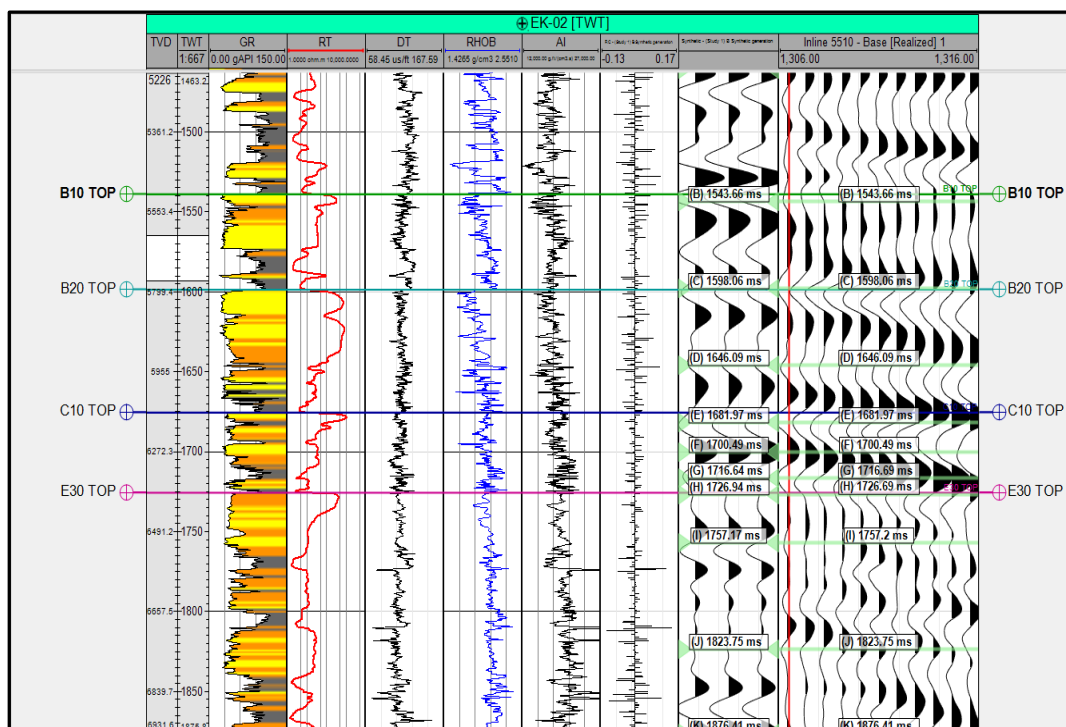


Figure 5: Well-to-Seismic Tie

III. Results and Discussion

Result Presentation

Time structure maps and depth structure maps of the horizon-B20 shows similar structural relationship and conformity. In the time map (Figure 7a) the anticlinal fault closure lies between the elevated time range of 1590 ms and 1610 ms TWT with a corresponding depth range of 5800 ftss to 5900 ftss in the depth map (Figure 7b), which is correlated with Sand B20 within the Agbada Formation. The depth map (Figure 7b) revealed the crest of the anticline at the depth of 5800ftss, which almost ties with what was obtained on the well logs. The anticline dip closure establishes the trap for the reservoir. Also, antithetic faults are growing and trending in the west-east direction as well as dipping in the direction. These closure which covers an appreciable area for a good prospect for hydrocarbon. Well EK2 is position at the crest of the anticlinal structure inbetween two assisted major fault trending east-west. It can be deduced from this study that the other wells were located to target the rollover anticline formed on the downthrown side of the growth fault. Trapping of hydrocarbons in an anticline is simply by means of closure which may be dependent or independent on faults. The rollover anticlines (red portions) are formed on the downthrown block of the growth fault, which indicate structural closure in these areas. The northern part of the study area controlled by the growth fault (major structure) characterized by an east-west trend and curved in shape that bound the field. Northern part of the study area can be seen as more prospect zone compared to the southern region because of anticlinal closure against the major fault forming a good structural trap.

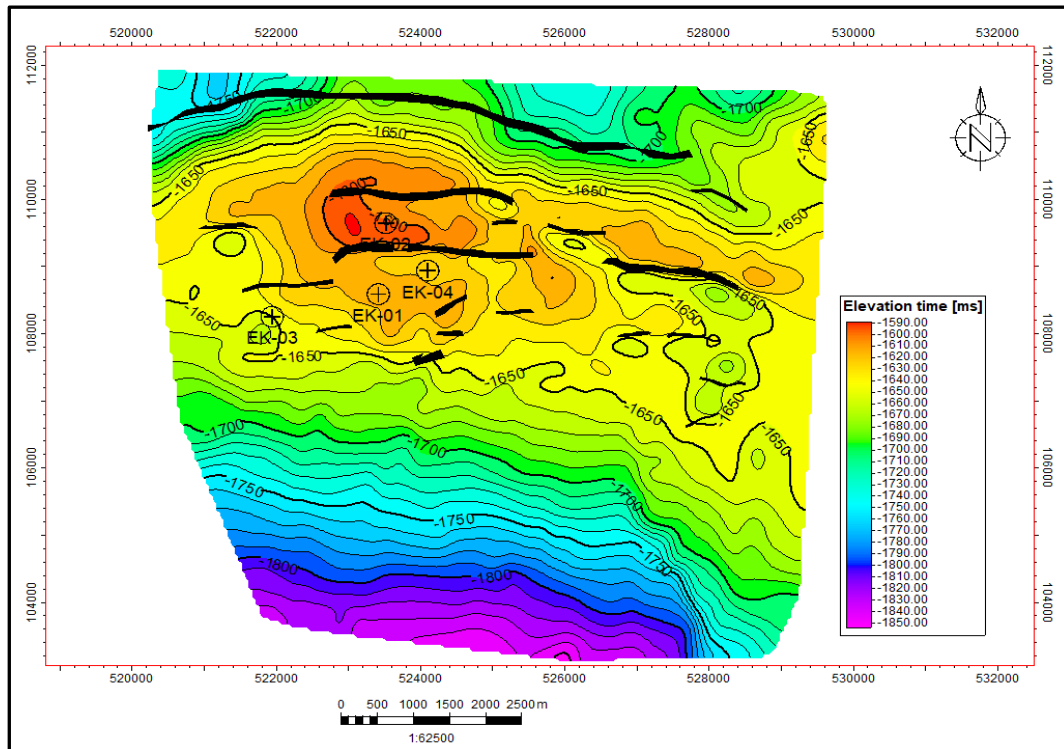


Figure 7a : Time map of the horizon-B20

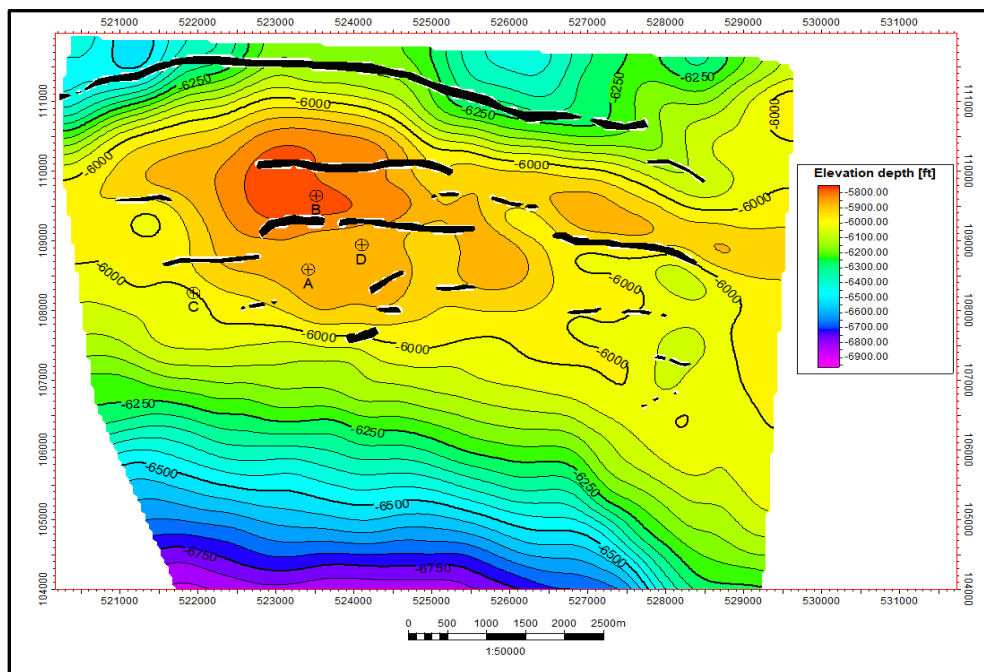


Figure 7b : Depth map of the horizon-B2

The RMS amplitude attribute extracted from the horizon-B20 (Figure 8) predicts variation in lithofacies across the sandstone body. The root mean square (RMS) amplitude map was also used to measure reflectivity in order to map the strongest direct hydrocarbon indicator which high indicates high amplitude close to the drilled wells and other areas away from well in the encircle eclipse zones. Amplitude maps generated for the mapped horizon complement the structural interpretation (structurally high locations). The encircle north east part of the field and region of downthrown block (northwest) where the wells are located is characterized by high amplitude which could be a bypassed prospective zones of hydrocarbon. Area around the fault anticlinal closure has similar amplitude strength like that of the downthrown thus making it a prospective zone for the drilling of development wells. The higher RMS amplitude indicates more lithological variation over the time

window. Higher RMS amplitude indicates better reservoir facies, especially when complimented with acoustic impedance.

(Figure 9) shows the model-based result of horizon B20 showing the acoustic impedance within the zone of interest. The Acoustic impedance result complement the structural maps and in turn with zones of anomalous amplitude which give credence to further interpretation of delineated hydrocarbon-bearing zones. The regions around the encircle eclipse is characterize with low acoustic impedance (16500g.ft/cm³.s - 18000g.ft/cm³.s) red-yellow colour. This low acoustic impedance is indicative of fluid-saturated sand (hydrocarbon).

The acoustic impedance sections were transformed into porosity section which indicate to the variation of porosity through the reservoir interval and shows the porosity increased in the uppermost part of the reservoir reached to 30% due to increasing of clean sand contain corresponding to low acoustic impedance. Moreover, the seismic porosity decrease toward the bottom of reservoir, as seen in Figure 10. The porosity maps shows enhance the porosity toward northeast part of study area of B20 horizon, while decrease toward southwest close to well 3.

The estimated petrophysical parameters of the study area are presented in tables 1.

Table 1. Showing estimated average petrophysical parameters for sand B20

Wells	Depth (ft)	Thickness (ft)	POROT (%)	VSH (%)	POROE (%)	K (mD)	Sw (%)
Wells EK1 B20 Top- B20 Base	5860 - 5965	105	31.1979	7.6493	28.9336	1362.98	27.5003
Well EK2 B20 Top- B20 Base	5796-5934	138	28.4713	8.6859	41.7388	12739.86	19.9196
Well EK3 B20 Top- B20 Base	5990-6106	116	32.1912	6.1756	30.3026	1477.338	25.8188

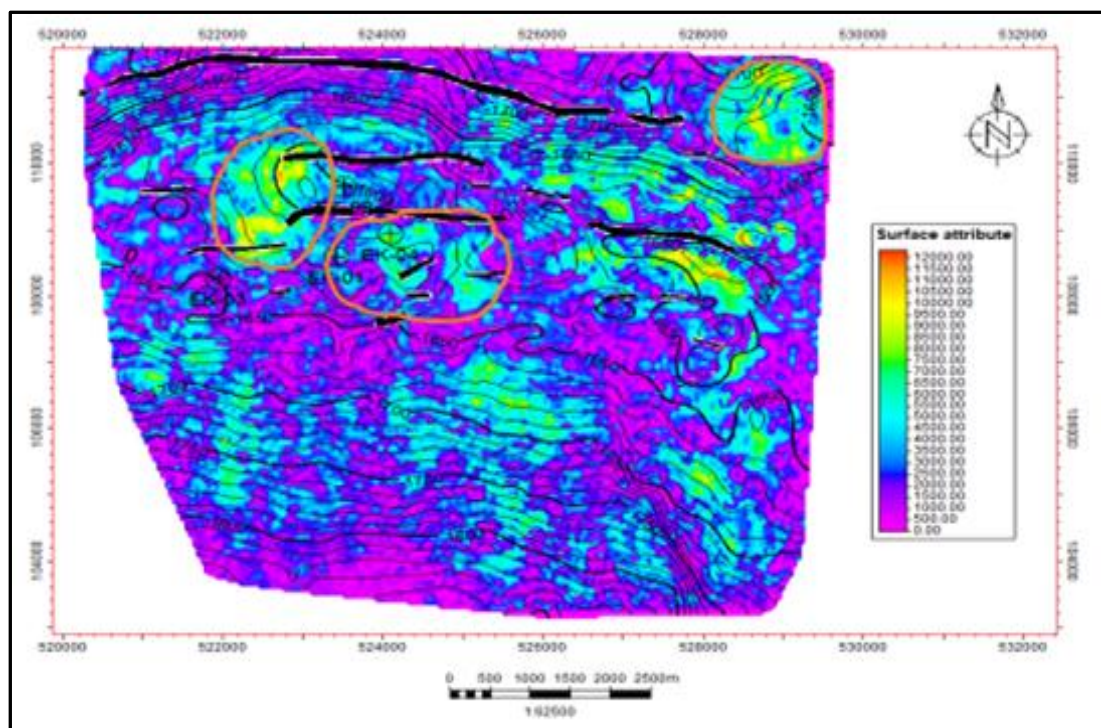


Figure 8: RMS Amplitude Attribute (B20)

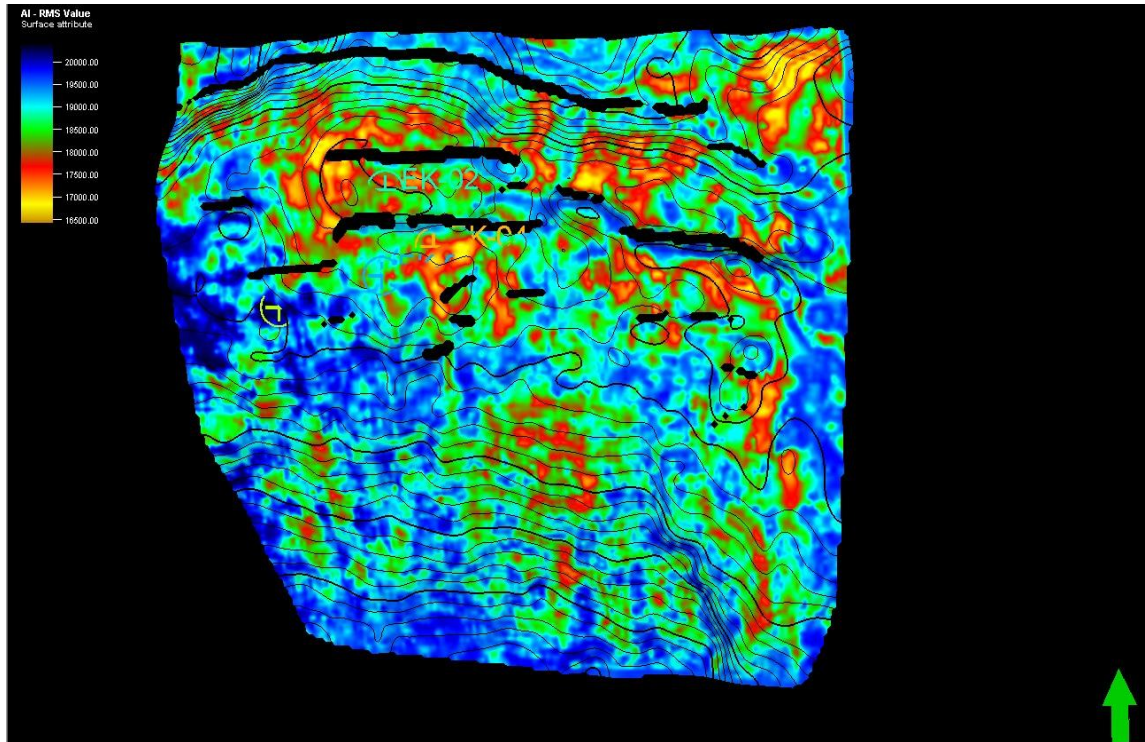


Figure 9: Seismic inversion surface B20

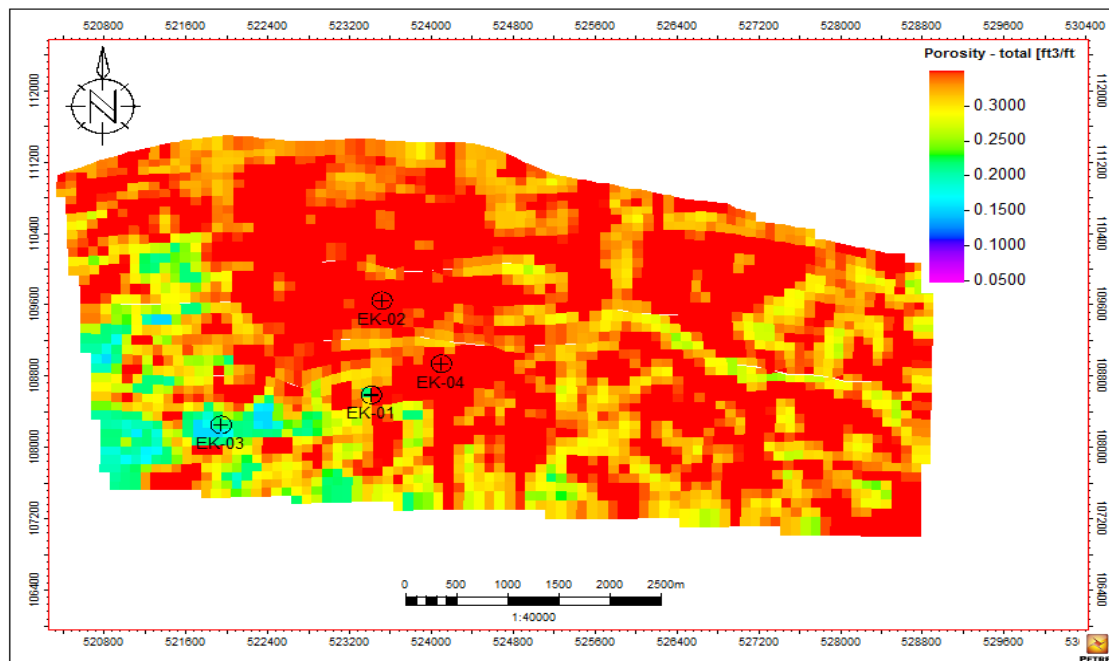


Figure 10: Seismic derived porosity for surface B20

IV. Discussion of Result

In this study, we have embarked on the delineation and mapping of hydrocarbon-bearing reservoirs from high reflectivity surface of the seismic sections and well logs within the depth interval of 5800ftss and 5910ftss. The time and depth maps horizon of interest picked demonstrated that the most predominant trap in Field was the crescentic growth fault. The hydrocarbons are transcendently trapped by rollover anticlines and fault closures in the Field. This structural trapping system accumulating hydrocarbon is a fault-dependent anticlinal structure since the strike of most of the mapped faults are situated close to the closures. However, for hydrocarbon to be present at well drilled on the structural high closures, the faults systems are most likely act as

sealing nature. This sealing faults results from high shale to sand ratio in the fault zone. The presence of impermeable shale within these zone prevents tertiary migration of hydrocarbon.

The RMS amplitude display maps reveals outstandingly strong reflection (bright spots) which may be indicative of reservoir rocks due to the presence of hydrocarbons in the identified sand. Amplitude pockets correlate with lithofacies variation, as high amplitude corresponds to sandy facies while low amplitude indicates shale contents. The drilled wells overlies low-amplitude zones probably because the pay sandstone is too thin to be resolved by the seismic data. Apart from the encircled eclipsed high amplitude zone (Figure 8) which are bypassed prospective zones, most of the extracted amplitudes at the wells do not conform to structure and hydrocarbon presence (direct hydrocarbon indicator, DHI); hence they are more related to lithofacies variation in this case (Bouvier *et al*, 1989). The implication is that reservoir sandstone is concentrated in the extremeNorth West and north east of the field close to the termination of major fault and along the flank of the anticlinal structure. These anomalous high amplitude bright spots observe in figure 8 coincides with defined area of low acoustics impedance in (Figure 9). The acoustic impedance map improved the interpretation for conceivable lithology segregation, thus, utilized as a key for separation of sand and shale facies. From the inversion results, acoustic impedance maps the horizon facies of sands of sands increased toward the north and northeast part of study area especially, at the top level of reservoir interval.

Low acoustic impedance areas indicate high porosity area. The porosity value of sandstone porous zone has average value 30%, these values agree with well logs. The most likely explanation is that porosity is a combination of depositional and diagenetic processes, with the diagenetic events destroying primary porosity. Because cleaner sandstones typically have greater original porosity than poorly sorted sandstones, we would expect to see higher predicted porosity in the high depositional-energy channels where percent sand content is higher than outside the channels. The porosity generally decreases with increase clay volume. The average value of water saturation of porous zone has 26.68%, primarily affected by their porosities.

V. Conclusion

Post-stack reflectivity inversion method and attribute analysis have been used to determine the prospectivity of reservoir structures and their acoustic effect in the Niger delta field. The petrophysical result shows estimated average porosity in B20 reservoir varies from 28% to 31% while the volume of shale and water saturation ranges from 6% to 8% and 19% to 27% in Niger Delta reservoir, respectively. The field is characterized by structural high and low features dominated by synthethic, antithetic growth faults and rollover anticlines. The seismic amplitude map (an interface property) interpreted complement the acoustic impedance which is a layer property utilized in characterizing the reservoirs in delineating lithofacies variation and associated fluid content in zone of interest. The results of the acoustic impedance inversion provides useful means of mitigating the risks associated with the exploratory efforts within the study area. This methodology can also be used for a quick evaluation of other reservoir properties.

Acknowledgement

The authors wish to thank World Bank, Africa Centre of Excellence, and University of Port Harcourt and also express their sincere thanks to the SHELL, Nigeria for access to their data.

References

- [1]. Adekanle, A., Enikanselu, P.A., 2013. Porosity Prediction from Seismic Inversion Properties over 'XLD' Field, Niger Delta. *Am. J. Sci. Ind. Re.* 4(1), 31-35.DOI:10.5251/ajsir.2013.4.1.31.35.
- [2]. Adepoju Y.O., Ebeniro J.O. and Ehirim C.N. 2013. DHI Analysis Using Seismic FrequencyAttribute On Field-AN Niger Delta, Nigeria. *IOSR Journal of Applied Geology and Geophysics (IOSR-JAGG)* e-ISSN: 2321-0990, p-ISSN: 2321-0982. Volume 1PP 05-10.
- [3]. Ali Aamir, Alves Tiago, Saad, FarhadAslam, Ullah, Matee, Toqeer, Muhammad and Hussain, Matloob 2018. Resource potential of gas reservoirs in South Pakistan and adjacent Indian subcontinent revealed by post-stack inversion techniques. *Journal of Natural Gas Science and Engineering* 49, pp. 41-55.
- [4]. Bouvier, J. D., Kaars-Sijpesteijn, C. H., Kluesner, D. F. and Onyejekwe, C. C., 1989. "Three-Dimensional Seismic Interpretation and Fault Sealing Investigations". *Nun River Field, Nigeria. AAPG bulletin.* 73(11): 1397 – 1414.
- [5]. Dagogo T., ChukwuemekaNgoziEhirim*, Joseph OnukansiEbeniro 2016. Enhanced Prospect Definition Using Well and 4D Seismic Data in a Niger Delta Field Geophysics Research Group, Department of Physics, University of Port Harcourt, Port Harcourt, Nigeria.
- [6]. Doyen, P. M., 1988, Porosity from seismic data—Ageostatistical approach: *Geophysics*, 53, 1263–1275.
- [7]. Evamy B.D., Haremboure J., Kamerling P., Knaap W.A., Molloy F.A., and Rowlands P.H.,1978. Hydrocarbon habitat of Tertiary Niger Delta: *American Association of PetroleumGeologists Bulletin*, v. 62, p. 1-39.
- [8]. Fontaine *et al.*, 1987, Seismic interpretation of carbonate depositional environments" (AAPG Bulletin).
- [9]. Hampson, D., Schuelke, J., and Quirein, J., 2001, Use of multiattribute transforms to predict log properties from seismic data: *Geophysics*,66, 220–236.
- [10]. Hart, B. S., and Balch, R. S., 2000, Approaches to defining reservoir Physical Properties from 3-D seismic attributes with limited well control: An example from the Jurassic Smackover Formation, Alabama:*Geophysics*, 65, 368–376.
- [11]. Krebs, J.R., Anderson, J.E., Hinkley, D., Neelamani, R., Lee, S., Baumstein, A., Lacasse, M.D., 2009.Fast full-wave field seismic inversion using encoded sources. *Geophys*, 74(6), WCC177-WCC188.DOL.org/10.1190/1.3230502

- [12]. Kumar, R., Das, B., Chatterjee, R., Sain, K., 2016. A methodology of porosity estimation from inversion of post-stack seismic data. *J. Nat. Gas Sci. Eng.*, 28, 356-364. DOI: 10.1016/j.jngse.2015.12.028.
- [13]. Latimer, R.B., Davison, R., Van Riel, P., 2000. Interpreter's guide to understanding and working with seismic derived acoustic impedance data. *Lead. Edge* 19 (3), 242–256.
- [14]. Pendrel, J., 2006. Seismic inversion—a critical tool in reservoir characterization. *Scand. Oil Gas Mag.* 5 (6), 19–22.
- [15]. Short, K.C., and Stäuble, A.J., 1967. Outline of geology of Niger Delta: American Association of Petroleum Geologists Bulletin, v. 51, pp. 761-779.
- [16]. Sinha, B., Mohanty, P. R., 2015. Post stack inversion for reservoir characterization of KG basin associated with gas hydrate prospects. *J. Ind. Geophys. Union* (April 2015). 19(2), 200-204.
- [17]. Reijers, T.J.A., Petters, S.W., and Nwajide, C.S., 1997. The Niger Delta Basin, in Selley, R.C., ed., *African Basins--Sedimentary Basin of the World 3*: Amsterdam, Elsevier Science, pp. 151-172.
- [18]. Stacher, P., 1995. Present understanding of the Niger Delta hydrocarbon habitat, in, Oti, M.N., and Postma, G., eds., *Geology of Deltas*: Rotterdam, A.A. Balkema, pp. 257-267.
- [19]. Thomas, C., 1995. Niger delta oil production, reserves, field sizes assessed: *Oil and Gas Journal*, November 13, 1995, pp. 101-103.
- [20]. Weber, K. J. (1971). "Sedimentological aspects of oil fields in the Niger delta," *Geologie en Mijnbouw*, vol. 50, pp.559–576.
- [21]. Weber, K.J., and Daukoru, E.M., 1975. *Petroleum geology of the Niger Delta: Proceedings of the Ninth World Petroleum Congress*, volume 2, Geology: London, Applied Science Publishers Ltd., pp. 210-221.

Ekone, N.O.et.al "Post-Stack Reflectivity Inversion for Hydrocarbon Prospectivity in the Niger Delta Field." *IOSR Journal of Applied Geology and Geophysics (IOSR-JAGG)*, 8(1), (2020): pp. 40-49.